Lab-on-a-Valve mesofluidic platform for on-chip handling of carbon coated titanium dioxide nanotubes in a disposable micro-solid phase extraction mode

María Teresa García-Valverde[a], María Rosende[b], Rafael Lucena[a], Soledad Cárdenas*[a], Manuel Miró*[b]

[a]*Departamento de Química Analítica, Instituto Universitario de Investigación en Química Fina y Nanoquímica IUIQFN, Universidad de Córdoba, Campus de Rabanales, Edificio Marie Curie, E-14071 Córdoba, España. E-mail: scardenas@uco.es. Tel: +34 957211066*

[b]*FI-TRACE Group, Department of Chemistry, University of the Balearic Islands, Carretera de Valldemossa, km 7.5, E-07122 Palma de Mallorca, Spain. E-mail: manuel.miro@uib.es, Tel: +34-971172746*

Abstract

Mesofluidic Lab-on-a-Valve (LOV) platforms have been proven suitable to accommodate automatic micro-solid-phase extraction approaches (µSPE) with on-chip handling of micrometer bead materials in a fully disposable mode to prevent sample cross-contamination and pressure drop effects. The efficiency of the extraction process notably depends upon the sorptive capacity of the material because the sorbent mass is usually down to 10 mg in LOV devices. Nanomaterials, capitalizing upon their enhanced surface to volume ratio and diversity of potential chemical moieties, are appealing alternates to microbead sorbents. However, the handling and confinement of nanomaterials in fluidic chip structures have been challenging to date. This is most likely a consequence of the aggregation tendency of a number of nanomaterials, including carbon-based sorbents that leads to excessive backpressure in flowing systems along with irreproducible bead loading. This article faces up these challenges by the *ad-hoc* synthesis of hybrid nanomaterials, such as porous carbon coated-titanium dioxide nanotubes (TiO_2-NT@pC). Tailoring of the surface polarity of the carbon coating is proven to foster the dispersion of TiO_2-NT@pC in LOV settings while affording a superior extraction capability of moderately non-polar species from aqueous matrixes. The determination of trace level concentrations of butylparaben (BPB) and triclosan (TCS) in seawater samples is herein selected as a proof-of-concept of the exploitation of disposable nanomaterials in LOV. The mesofluidic platform accommodating µSPE features on-line hyphenation to LC-MS/MS for reliable determination of the target

analytes with excellent limits of detection (0.5 and 0.6 ng/L for BPB and TCS, respectively) and intermediate precision (relative standard deviation < 5.8 %). Using 5.0 mL of sample and 200 μL of eluent, enrichment factors of 23 and 14 with absolute extraction efficiencies of 90 ± 14 % and 58 ± 8 % for BPB and TCS, respectively, were obtained. The relative recovery values of 107 % (BPB) and 97 % (TCS) in seawater demonstrate the applicability of on-line LOV-LC-MS/MS method using TiO_2-NT@pC for handling troublesome environmental samples.

Sample treatment, a critical step in many analytical methodologies, normally consumes around 60-80% of the total analysis time and a considerable amount of consumables. It is also a source of systematic errors, notably in case of non-automatic or partially mechanized procedures. Automation and miniaturization of assays (e.g. involving flow-based methodology) give rise to improved analytical quality of the final results while fostering time and resources saving [1-3]. Capitalized upon a mesofluidic monolithic structure placed atop a multiposition rotary valve, Lab-on-valve (LOV) platforms, tagged as the third generation of flow injection analysis [4-7], are of undisputed interest in this context. Though LOV was conceived to accommodate a wide variety of wet-chemical assays based on programmable flow control by user-friendly software, further extension to automating sample preparation approaches has been proven feasible [8-11]. The channel geometry allows LOV devices to be used as platforms for the so-called *bead injection* (BI) approach [12-14] consisting on *in-situ* generation of micro-solid phase extraction (μSPE) columns, trapped on-chip by a mechanical restrictor, with automatic on-line disposal of the sorbent material after every individual sample or sample cohort analysis as ruled by the matrix complexity [8-15]. The idea behind is to offset backpressure and cross-contamination effects occurring on flow-through SPE modes with reusable packed columns. Sorbent materials in LOV manifolds are usually recommended to be homogeneous in particle size, of micrometer range ($\geq$ 30 μm) and of spherical shape for facile *in-line* handling and repeatable packing and unloading from the mesochannels [5]. Commercial micrometer-sized bead sorbents, such as, Sephadex, Sepharose Fast Flow, aldehyde-laden Aminolink and Cytopore as cell microcarriers, as well as some polymeric phases including divinylbenzene-co-N-vinylpyrrolidone (Oasis HLB), hydroxylated copolymers (Bond Elut Plexa) and the like have been up to now the sorbents of choice in LOV settings [9, 10, 13].

Over the past decade, carbon-based nanomaterials [16-20] including carbon nanotubes (CNTs), graphene, fullerene C_{60}, carbon nanohorns and carbon nanodiamonds, among others, have gained heightened interest in analytical science as a consequence of their feasibility of uptaking and preconcentration of organic molecules by hydrophobic interactions, π-π stacking, hydrogen bonding, and electrostatic effects [19]. CNTs are, by far, the carbon-based nanomaterials of choice in sample extraction [21] for enrichment and preconcentration of legacy and emerging organic contaminants [22, 23]. The main issue is the fact that the entanglement and aggregation tendency of CNTs hinder their applicability in flow-through sorptive procedures because of the

progressively tighter packing of the carbon nanomaterials and the increase in pressure drop, as signaled by Abdel-Rehim and co-workers in a recent comprehensive review article [21]. In fact, the aggregation phenomena lead to significant decrease of active surface for sorption. Over the years, a number of chemical and physical methods have been proposed to tackle this problem including (i) the dynamic coating of CNTs with surfactants or polyelectrolytes [24-26], (ii) the functionalization or surface decoration with chemical moieties [27, 28] and (iii) the application of external energy sources (e.g. ultrasound irradiation) [29], all aimed at ameliorating the dispersability of CNTs in aqueous media. Alternatively, novel designs of column systems [30], the blending of CNTs with inert materials in packed columns [31] or the use of stirred-flow mini-reactors for holding and dispersing of CNTs [32] helped alleviate the flow impedance of CNTs in flow-through SPE settings. Carbon coating of distinct core materials (e.g. metallic oxide nanoparticles) has however emerged as a viable alternative that combines the features of the raw nanomaterial with the additional aforementioned advantages of carbon nanoentities [33]. For example, carbon coated titanium dioxide nanotubes (TiO_2-NT@C) have demonstrated superior aqueous dispersability, and enhanced extraction capability of moderately non-polar species [34], as compared to raw CNTs, due to the presence of some residual hydroxyl, carbonyl or carboxylic moieties on their surface, which are tailorable with control of the synthesis temperature [35].

This article reports the utilization of nanomaterials (porous TiO_2-NT@C (TiO_2-NT@pC)) for on-line automatic micro-SPE in disposable mode using the determination of low abundance triclosan (TCS) and butylparaben (BPB) in troublesome samples (e.g. seawater) as a proof of concept applicability. To the best of our knowledge, this is the first work dealing with carbon-based nanoparticles in LOV, which opens new opportunities for *in-line* handling of nanomaterials in mesofluidic platforms.

EXPERIMENTAL

Detailed information of chemicals and samples as well as the synthetic procedures for TiO_2-NT, TiO_2-NT@C and TiO_2-NT@pC and physicochemical characterization thereof are available as Supporting Information (SI).

Analytical instrumentation

The mesofluidic manifold consisted of a micro-sequential injection system (μSI, FIAlab Instruments, Bellevue, Washington, USA) composed of a 3000-step bi-directional

syringe pump (Cavro, Sunnyvale, USA) furnished with a 5 mL gas-tight glass syringe (Cavro) for automatic fluid handling, a three-way distribution valve at its head, which allowed connection with either the manifold or the carrier (water) solution, and an eight port selection valve (Vici Valco, Schenkon, Switzerland) on top of which it was mounted the mesofluidic LOV conduit platform. The LOV microbore assembly (1 cm thick and 6.5 cm external diameter, FIAlab instruments), fabricated from chemically resistant polyetherimide (ULTEM), encompassed eight integrated microchannels (1.0 mm i.d./29 mm length) whose connection with the multi-port valve was enlarged to 1.7 mm i.d. For the sake of clarity, a schematic description of the LOV manifold is shown in Fig. 1.

The central port in LOV was connected to a holding coil (HC) made of 300 cm × 1.5 mm ID fluoropolymer (PFA) tubing. The microchannel connecting the central port with port 1 serves as a microcolumn position for the renewable/disposable TiO_2-NT@pC nanoparticles into which a cotton fabric plug was inserted to trap the sorbent while allowing the fluids to flow freely. Nanoparticle suspensions were prepared by dispersing TiO_2-NT@pC in pure methanol, and kept in a 2 mL-polypropylene syringe mounted vertically on port 5 in the LOV. The eluent (90:10 (v/v) methanol:water) and the cleansing solvent (Milli-Q water adjusted to pH 1.5) reservoirs were attached to peripheral ports 3 and 7 of the LOV, respectively, whereas port 4 was employed for air aspiration with the purpose of liquid segmentation and assistance in the on-line dispersion of the nanosorbent pending aspiration into the chip platform. Port 6 was utilized for sample introduction into the flow system. The outlet of the LOV microcolumn is via a 100 cm × 0.8 mm ID PTFE tubing hyphenated to the 6 port-injection stainless steel valve of an HPLC equipment (Agilent 1260, Agilent, Palo Alto, CA) for on-line heart-cut analysis of the eluate.

The freeware Cocosoft 4.3 software package written in Python [36] and the extensions thereof were used for user-friendly control of the µSI setup, *namely*, LOV/multi-port valve position, direction and flow rate of the syringe pump and head valve position.

In the optimization of the on-chip LOV-based µSPE procedure and method validation, off-line analyses of the SPE eluates were performed by resorting to Jasco AS-4050 HPLC system (Jasco, Easton, MD). The HPLC module was equipped with a quaternary pump (PU-4180-LPG model, < 700 bar), an integrated 60-position autosampler, a photo-diode array detector (PDA, MD-4017 model) and a Kinetex C18-core shell (150 × 3 mm ID, 2.6 µm) chromatographic column preceded by a C18-security guard ultra-

cartridge (2× 3 mm ID, part no. AJO-8775) all from Phenomenex (Torrance, CA). The mobile phase consisted of (A) water and (B) 90:10 (v/v) methanol:water at a flow rate of 0.6 mL/min using a gradient elution program. The initial eluent composition was fixed at 50 % B, increased to 100 % B in 2.5 min, kept during 3 min, and finally returned to the initial gradient conditions. The chromatogram run lasted 11 min, with retention times of 2.2 min and 5.2 min for BPB and TCS, respectively. The injection volume for off-line detection experiments was 25 µL using a partially filled stainless-steel loop. The PDA detector was programmed to cover the UV region from 200-400 nm, with analytical wavelengths of 210 nm and 254 nm for TCS and BPB, respectively, using ChromNAV 2.0 software for peak area integration.

For real sample analysis and on-line measurements, the µSI-LOV system was hyphenated to Agilent 1260 Infinity HPLC-MS system. The HPLC is marketed with a two-grooves seal rotor, so this had to be changed by a three-grooves seal rotor for ease of connection of the µSI-LOV setup to HPLC. Chromatographic separation was accomplished by reversed-phase separation on Zorbax Eclipse XDB-C18 (150 × 4.6 mm ID, 5 µm) chromatographic column from Agilent using 90:10 (v/v) methanol: 0.2% (v/v) ammonia at 0.3 mL/min (for better synchronization with the LOV sample processing method) in isocratic mode. The chromatographic run lasted 10 min, with retention times of 6.6 min and 7.7 min for BPB and TCS, respectively. An in-line filter (0.2 µm, 2.1 mm ID), also from Agilent, was selected as a pre-column to preserve the integrity of the analytical column. The HPLC injection valve was furnished with a 300 × 0.8 mm ID loop of ca. 150 µL. The injection program of the HPLC was set to switching the rotary injection valve from ‘load’ to ‘inject’ for the on-line eluate from the LOV to be analyzed in a time-controlled heart-cut bi-dimensional mode. Quantification was performed on Agilent 6420 Triple Quadrupole MS with electrospray source using Agilent MassHunter Software (version B.06.00) for data analyses. The mass spectrometer settings were fixed aiming at improving the SRM signal. The flow rate and the temperature of the drying gas (N_2) were 9 L/min and 250 °C, respectively. The nebulizer pressure was 29 psi, and the capillary voltage was kept to 4000 V in positive mode. Full scan and MS/MS spectra of TCS, TCS-D3, BPB and BPB-^{13}C were obtained by direct infusion of 1 mg/L of the standards in methanol. Both analytes and ISs were detected by SRM transitions. The SRM parameters for the target analytes and isotopologues of this study are specified in Table S1.

Mechanized analytical procedure

The operational sequence for automatic separation and preconcentration of TCS and BPB in seawater by the proposed LOV-μSPE method is breakdown in four main steps, *viz*.: (i) TiO_2-NT@pC uptake into LOV, nanomaterial trapping and conditioning, (ii) sample loading and clean-up to remove unwanted matrix components, (iii) elution of the analytes and (iv) in-line renewal of the beads by disposal to waste after every individual assay. Before each step, a given volume of air (usually 100 μL, unless otherwise stated) is aspirated into the HC in order to preserve the integrity of the aspirated plug solution and circumvent axial/longitudinal dispersion of the individual solutions into the carrier. The onset of the automatic method involves the sequential aspiration of 400 μL of air and 200 μL of methanol into HC followed by flow-reversal pumping at high flow rate, viz., 20 mL/min, toward port 5 (syringe body containing TiO_2-NT@pC) for *in-situ* generation of the nanomaterial suspension. This step facilitates further drawing of TiO_2-NT@pC into the LOV by software-controlled flow programming. In brief, once the nanotubes are dispersed, 200 μL of dispersed medium are taken from port 5 into HC at 1000 μL/min and then directed to port 1 at 500 μL/min for confinement of the TiO_2-NT@pC microcolumn. Under the above experimental conditions, the LOV integrated sorbent column contained a sorbent mass of 3.9 ± 1.4 mg (n = 30). Prior to sample loading, the TiO_2-NT@pC microcolumn is rinsed subsequently with 500 μL of methanol and 500 μL of water at pH 1.5 at 500 μL/min for sorbent conditioning. The syringe pump is then programmed to bring 5 mL of sample through the TiO_2-NT@pC packed sorbent at 500 μL/min. The LOV microcolumn is then rinsed with 1000 μL of carrier at 500 μL/min to remove non-retained, unwanted material from the sample matrix. The elution step is undertaken at 500 μL/min using 200 μL of 90:10 (v/v) methanol:water. A given volume of carrier, namely, 450 μL, was subsequently pumped to bring the eluate to the injection loop for a heart-cut injection mode (injection volume = 150 μL). The idea behind of the heart-cut analysis is to minimize peak broadening effects while improving chromatographic resolution. The operation of LC-MS/MS initializes manually whenever the analytes of the first sample are being eluted from the LOV platform. The injector program of the Agilent MassHunter Software was configured to turn the valve from the inject to the load position for 2 min so as to trap the eluate plug. Thereafter, the valve is switched back to the inject position whereupon the HPLC analysis of the eluate is initialized. Prior to the next sample or replicate analysis, the HC is cleaned with carrier to minimize analyte carryover. To finalize the

on-line µSPE protocol, after every single individual assay, the TiO_2-NT@pC microcolumn is discarded by aspirating the sorbent previously soaked with 1.0 mL of 90:10 (v/v) methanol:water at 1000 µL/min into HC for further withdrawal to waste. The latter was repeated two-fold to assure that the remaining TiO_2-NT@pC nanoparticles are entirely removed from LOV mesoconduits, central port of the rotary valve, and HC as well. For the sake of comprehension of the automatic protocol for manipulation of the TiO_2-NT@pC nanoparticles in the LOV structure, a video sequence is available as SI.

RESULTS AND DISCUSSION

Characterization of the nanomaterials for sorptive microextraction

The morphology of the in-house synthesized materials, *namely*, TiO_2-NT@C and TiO_2-NT@pC, was evaluated by TEM images. Both nanomaterials feature similar lengths and dimensions, as shown in Fig. S1, with an average diameter of 5 nm and lengths ranged from 100 to 400nm. The surface area of TiO_2-NT@pC is 219.62 m^2/g against 170.87 m^2/g presented by TiO_2-NT@C, representing an increase of 24 % corresponding to the synthesis enhancement. It should be born in mind that the addition of CTAB throughout the TiO_2-NT@pC synthesis avoids the formation of a seamless caramel shield thereby increasing the extent of pores of smaller dimensions. The zeta potential (Z) measurements are of particular interest as to shed light onto the surface polarity of the nanomaterial. An increase in surface polarity fosters excellent dispersability of the sorbent yet hinders the interaction with the hydrophobic target analytes under dynamic flow-through extraction conditions. On the other hand, a low polarity makes the dispersion inefficient for a repeatable packing and withdrawal of the nanomaterials in LOV settings. It should be born in mind that $Z > 30$ mV or < -30 mV are indicative of a good stability of the nanomaterial dispersion. The Z of TiO_2-NT@pC at pH 1.5 (sample pH during the extraction step) is 20 mV. The agglomeration of the nanomaterial is thus circumvented in the time course of sample loading through the LOV microcolumn. However, the Z in methanol is a mere -6.98 mV making the *in-situ* generation of the nanomaterial suspension within the external container necessary prior to aspiration into LOV to ensure a reproducible automatic packing of the nanoparticles in the mesoconduits.

The extraction performance of the two carbonaceous TiO_2-NT materials was thoroughly evaluated and compared against commercially available sorbents including activated carbon, C_{18}-octadecyl modified silicagel and co-polymeric Oasis HLB in a batchwise dispersive μSPE mode [34] described in SI and illustrated in Fig. S2. The sorption efficiency, calculated on the basis of the non-retained amount of compounds in the sample effluent, gave insight into the magnitude of the distribution coefficients (K_d) for the target analytes in aqueous environments. As can be seen in Fig 2A, activated carbon (AC) provided the best results followed by Oasis HLB and TiO_2-NT@pC. The TiO_2-NT@C notwithstanding of its good dispersibility (Z= 23 mV at pH 1.5) yielded poorer retention efficiency for both analytes (< 45%) as compared to TiO_2-NT@pC (> 75%) as a consequence of the limited specific surface. For conventional C_{18}-silicagel micrometer beads, extraction efficiency < 60% was observed for the most polar substance, viz., BPB. Further, the handling of non-spherical C_{18} bead chunks in LOV platforms [15, 37] as renewable entities was troublesome as a result of poor dispersability and tendency to settle within the LOV channels, making the on-line disposable μSPE method impracticable.

For further critical comparison among sorbent entities for elucidating their suitability in a miniaturized LOV-SPE format, the elution profiles of both analytes are depicted in Fig. 2B. Negligible amounts of BPB and TCS were eluted from activated carbon in a reasonable volume of methanolic eluent because of the high K_d values. This makes activated carbon useless in a mesofluidic LOV-μSPE mode with on-line hyphenation to LC-MS/MS. The TiO_2-NT@pC and Oasis HLB sorbents afforded similar elution profiles for BPB, with no statistically significant differences (α=0.05) between the extraction recoveries within the first elution plug (150 μL eluent) for both sorbents (t_{exp} =0.77 vs $t_{crit(0.05;\,4)}$=2.77). However, the shaper elution profile of TiO_2-NT@pC for the less polar contaminant, *viz*., TCS, indicates a better performance against Oasis HLB in on-line LOV-μSPE mode, which is supported by a 2-fold improved overall extraction performance (see Fig. 2C). The chromatograms of the first eluate fraction (E1: 150 μL) for both analytes throughout the various evaluated sorbents are illustrated in Fig. S3.

Because of faster elution and improved extraction performance of TiO_2-NT@pC against Oasis HLB sorbent for TCS, the former nanosorbent material was selected for further studies in an LOV format.

Optimization of the LOV-μSPE method with renewable TiO_2-NT@pC nanosorbent

Considering the fact that one-at-a-time univariate methods do not necessarily provide comprehensive evaluation of experimental systems, the analyte extraction efficiency was investigated in our miniaturized setup using a two-level full factorial multivariate design (2^3+3 center points). A detailed description of the multivariate optimization protocol is available as SI. The sample volume, the loading flow rate, and the ionic strength were selected as the main factors, with the extraction efficiency, calculated as the ratio of eluate to loaded analyte mass, as the analytical response (see Table S2). The sample volumes ranged from 1 to 5 mL as a trade-off between enrichment factor and sample throughput, and the sample flow rates spanned from 0.5–1.0 mL/min on the basis of preliminary experiments that revealed the absence of pressure drop using standard solutions within that experimental domain. The range of 0-3.5 (w/v, %) NaCl for the ionic strength variable was selected aimed at evaluating potential breakthrough effects in seawater samples, with the highest level of the factor mimicking the salt composition in seawater.

The statistical significance of the effect of the main factors and their second-order interactions upon the extraction efficiency for BPB and TCS was evaluated by ANOVA. The standardized factor effects could be facilely visualized by Pareto charts. These are histograms in which the length of each bar is proportional to the value of an experimental *t* value calculated for every individual factor. A given effect is considered significant with regard to the extraction efficiency when its *t experimental* value is ≥ *t critical* at a 0.05 significance level, which is set as the benchmark in the chart, and corresponds, in our case, to 2.78 for four degrees of freedom. The standardized effects may be positive (grey) or negative (blue), which in turn stand for the improvement or decrease of the extraction yield, respectively, when the specific factor increases from the lowest to the highest coded level. The Pareto chart (Fig. 3) revealed that neither the sample flow rate nor the sample volume are significant effects upon the extraction efficiency of both analytes. On the contrary, the sample ionic strength is deemed significant for TCS, the greater the electrolyte concentration the lower the extraction/elution efficiency was. It should be noted that the polarity of the carbon surface might be enhanced by the occurrence of electrolytes, thus excluding the more hydrophobic species. The salt content of the sample also increases sample viscosity, which could detrimentally affect the extraction rate under dynamic flow-through

conditions in LOV approaches. The lack-of-fit test was undertaken to elucidate whether the selected first-order model is adequate to describe the experimental data. The test is performed by comparing the variability of the residuals of the first order model against those of the replicate settings of the center point. Because the calculated P-values of 0.501 and 0.102 for TCS and BPB, respectively, are greater than 0.05, this model appears to be adequate for the observed data at the 95% confidence level with no need of undertaking second-order quadratic (surface response) models.

Aimed at detecting the lowest possible concentrations of our target pollutants in seawater, the sample volume was fixed to 5 mL with a sample loading flow rate of 0.5 mL/min to prevent the potential occurrence of flow backpressure in real sample analysis. Because there is a statistically significant dependence of the retention efficiency of TCS upon the sample ionic strength, a matrix-matched calibration in 3.5% (w/v) NaCl was used throughout for unbiased quantification of TCS in seawater samples.

Analytical figures of merit

Using the selected experimental conditions for the automatic LOV-TiO_2-NT@pC micro-extraction process, the analytical method hyphenated on-line to LC-MS/MS was validated in terms of dynamic linear range, limits of detection (LOD), intermediate precision, absolute recovery, enrichment factor and lack of bias (trueness). The dynamic linear range was assessed at six concentration levels and spanned from 1.7 to 250 ng/L and 2.0 to 250 ng/L for BPB and TCS, respectively, using matrix-matched calibration curves ($R>0.9984$). The LODs and LOQ calculated at the S/N=3 and S/N=10 level, respectively, were 0.5 ng/L and 1.7 ng/L, and 0.6 ng/L and 2.0 ng/L, for BPB and TCS, respectively. The intermediate precision was evaluated as the relative standard deviation (RSD) of three replicates at three distinct concentration levels, namely: 50, 100 and 250 ng/L. The RSDs spanned from 1.1-3.5 % and 1.9-5.8% for BPB and TCS, respectively, using in-line disposable TiO2-NT@pC. Intermediate precision for handling of nanoparticles in our LOV setup is even better to that previously reported for spherical micrometer beads in LOV with RSD > 10 % [38,39], which is attributed to the offset of differences in the amount and packing characteristics (aspect ratio, void volume, etc…) of the sorbent microcolumns with the utilization of isotopologues.

Absolute percent recoveries (R_{abs}) in surrogate seawaters obtained under optimum physicochemical experimental conditions were 90 ± 14% and 58 ± 8% for BPB and TCS, respectively. The enrichment factors (E_f) calculated as:

$$E_f = \frac{V_{sample}}{V_{eluate}} \times \frac{R_{abs}}{100}$$

were 23 and 14 for BPB and TCS, respectively.

To evaluate the feasibility of a matrix matched calibration using saline water, viz., 3.5 % (w/v) NaCl, the method of the standards addition with real seawater samples as indicated in Experimental (spike range: LOQ - 250 ng/L) was compared against the calibration graph with surrogate seawater using a *t*-test for comparison of slopes [40]. Statistical calculations are available as Supporting information. Because in all instances $t_{exp} < t_{crit}$, no statistically significant differences between the matrix-matched calibration and the standard addition method in seawater were observed for either analyte, thereby indicating the suitability of the surrogate matrix for the LOV-µSPE-LC-MS/MS system. A seawater chromatogram for BPB and TCS following on-line LOV-µSPE is illustrated in Fig S4.

The lack of bias (method trueness) [41,42] was corroborated by spike recoveries of freshly collected seawater. Five samples were analysed (see Experimental) with concentrations of BPB and TCS < LOQs in all instances except for one sample in which the concentration of TCS was 8.7 ± 1.8 ng/L. Aliquots of a seawater sample were then spiked at three concentration levels, namely, 50, 100 and 250 ng/L and analysed by the LOV-µSPE-LC-MS/MS method. The average relative recoveries of the spiked seawater aliquots for BPB and TCS were 107 % and 97 %, respectively.

In our work, the potential reuse of the nanosorbent in the LOV was not applicable due to the progressive build-up of backpressure in the analysis of undiluted seawater whereby the exploitation of the on-line disposable approach for single-use automatic µSPE was deemed imperative. Potential sample cross-contamination effects in the miniaturized packed column were also circumvented.

The analytical figures of merit of the proposed LOV-TiO_2-NT@pC-LC/MS/MS method are compared in Table 1 against those of previous methods in the literature [43-53] for determination of trace levels of parabens and TCS in distinct surface waters including seawater, lake and river water. In a previous article dedicated to seawater analysis [43], a poorer detection limit for BPB (23.2 ng/L vs 0.5 ng/L in this work) was reported notwithstanding harnessing to MS detection and a six-fold increase in sample volume. Our method also features improved absolute recovery (90 ± 14 % vs 51.6 %) and better precision for BPB (3.5% vs 12%) than those reported in previous procedures [52] because of the mechanization of the overall sample pretreatment step with the

subsequent elimination of sources of uncertainty. It should be stressed the fact that a vast number of scientific publications reporting the determination of parabens and TCS in environmental waters do analyze less troublesome samples, such as tap, river and lake water [44-51,53] with sample volumes up to 1000 mL [49,51] which made the automation of the analytical protocol impracticable. Notwithstanding the large volumes of sample processed, our LODs fall inside the range of LODs of the abovementioned methods (0.01–40 ng/L) [43,44,46,47,49-51,53]. In fact, using exactly the same sample volume as the one herein selected (5 mL sample), significantly poorer LOD for TCS, namely, 2-580 ng/L [45,48] were previously reported. The applicability of the proposed LOV-TiO_2-NT@pC platform as a front end to LC/MS/MS for the determination of TCS and BPB in seawater is fully corroborated on the basis of the reported occurrence levels of TCS and BPB in seawater spanning from 16.2 to 99.3 ng/L [54] and from 0.2 to 7.1 ng/L [55] for TCS and BPB, respectively.

CONCLUSIONS

This article describes for the first time the use of carbon coated nanoparticles as on-chip disposable sorbents for μSPE in a LOV mode. Because of the aggregation tendency of carbon nanomaterials, applicability as sorbents in flow-through SPE settings is rather scarce and their handling as renewable entities in micro/mesofluidic platforms has been deemed a daunting task. Here we have demonstrated that TiO_2-NT@pC overcomes this limitation. The tubular shape of TiO_2-NTs provides a high surface to volume ratio while the carbon coating plays a double role: The hydrophilic/hydrophobic balance of the carbon coating, which can be tuned with the synthesis temperature, allows facile dispersability on aqueous media and fosters good sorption capacities for both non-polar and moderately polar organic species.

The hyphenation of LOV and LC-MS/MS has been proven suitable for the determination of TCS and BPB in seawater as a proof-of concept applicability for determination of both pollutants at the low ppt-level with RSD < 6 % using renewable sorptive nanoentities with relative recoveries of 107 % and 97 % for BPB and TCS, respectively. Further work is underway for scale-up applicability of on-line LOV-TiO_2-NT@pC-LC-MS/MS analysis of contaminated seafood commodities and untargeted determinations of trace level concentrations of emerging contaminants in the marine environment.

Acknowledgments

Financial support from the Spanish State Research Agency (AEI) through projects CTQ2014-52939R (AEI/FEDER, UE); CTM2014-56628-C3-3-R (AEI/FEDER, UE), CTM2014-61553-EXP (AEI/FEDER, UE), CTM2017-84763-C3-3-R (AEI/FEDER, UE) and CTQ2017-83175R (AEI/FEDER, UE) is gratefully acknowledged. M. T. García-Valverde expresses her gratitude for her PhD scholarship (Refs. BES-2015-071421) from the Spanish Ministry of Education. The authors would like to thank the Central Service for Research Support (SCAI) and the Instituto Universitario de Investigación en Química Fina y Nanoquímica (IUIQFN) of the University of Córdoba. The authors are also grateful to Dr. David J. Cocovi-Solberg for his assistance throughout the automatic assays using Cocosoft freeware.

References

[1] Ríos, A.; Escarpa, A.; Simonet, B. Miniaturization of Analytical Systems: Principles, Designs and Applications, 1st ed.; Wiley-VCH Verlag, Weinheim, 2009.

[2] Trojanowicz, M. Advances in Flow Analysis, Wiley-VCH Verlag, Weinheim, 2008.

[3] Trojanowicz, M.; Kołacińska, K. *Analyst* **2016**, 141, 2085-2139.

[4] Quintana, J.B; Boonjob, W.; Miró, M.; Cerda, V. *Anal. Chem.* **2009**, 81, 4822-4830.

[5] Miró, M.; Hansen, E. *Anal. Chim. Acta* 2007, 600, 46-57.

[6] Hansen, E. H.; Miró, M. *Trends Anal. Chem.* **2007**, 26, 18-26.

[7] Miró, M.; Hansen, E. H. *Appl. Spectrosc. Rev.* **2008**, 43, 335–357.

[8] Yu, Y.; Jiang, Y.; Chen, M.; Wang, J. *Trends Anal. Chem.* **2011**, 30, 1649-1658.

[9] Luque de Castro, M.D.; Ruiz-Jiménez, J.; Pérez-Serradilla, J.A. *Trends Anal. Chem.* **2008**, 27, 118-126.

[10] Miró, M.; Hansen, E. H. *Anal. Chim. Acta* **2012**, 750, 3–15.

[11] Vidigal, S. S. M. P.; Toth, I. V.; Rangel, A. O. S. S. *Anal. Methods* **2013**, 5, 585–597.

[12] Miró, M.; Kradtap-Hartwell, S.; Jakmunee, J.; Grudpan, K.; Hansen, E. H. *Trends Anal. Chem.* **2008**, 27, 749–761.

[13] Miró, M. *Trends Anal. Chem.* **2014**, 62, 154–161.

[14] Miró, M.; Oliveira, H. M.; Segundo, M. A. *Trends Anal. Chem.* **2011**, 30, 153–164.

[15] Miró, M.; Jonczyk, S.; Wang, J.; Hansen, E. *J. Anal. At. Spectrom*. **2003**, 18, 89-98.

[16] Scida, K.; Stege, P.; Haby, G.; Messina, G.; García, C. *Anal. Chim. Acta* **2011**, 691, 6-17.

[17] Zarei, M.; Zarei, M.; Ghasemabadi, M. *Trends Anal. Chem.* **2017**, 86, 56–74.

[18] Justino, C. I. L.; Gomes, A. R.; Freitas, A. C.; Duarte, A. C.; Rocha Santos, T. A. P. *Trends Anal. Chem.* **2017**, 91, 53–66.

[19] Pyrzynska, K. *Trends Anal. Chem*. **2013**, 43, 100-108.

[20] Lasarte-Aragonés, G.; Lucena, R.; Cárdenas, S.; Valcárcel, M. *Bioanalysis* **2011**, 3, 2533-2548.

[21] Ahmadi, M.; Elmongy, H.; Madrakian, T.; Abdel-Rehim, M. *Anal. Chim. Acta* **2017**, 958, 1-21.

[22] Cai, Y.; Jiang, G.; Liu, J.; Zhou, Q. *Anal. Chem*. **2003**, 75, 2517–2521.

[23] Wang, J.; Jiang, D.; Gu, Z.; Yan, X. *J. Chromatogr. A* **2006**, 1137, 8-14.

[24] Strano, M.; Moore, V.; Miller, M.; Allen, M.; Haroz, E.; Kittrell, C.; Hauge, R.; Smalley, R. *J. Nanosci. Nanotechnol.* **2003**, 3, 81-86.

[25] Du, Z.; Yu, Y.-L.; Wang, J.-H. *Anal. Bioanal. Chem.* **2008**, 392, 937–946.

[26] Springer, V. H.; Lista, A. G. *Talanta* **2010**, 83, 126–129.

[27] Mitchell, C.; Bahr, J.; Arepalli, S.; Tour, J.; Krishnamoorti, R. *Macromolecules* **2002**, 35, 8825-8830.

[28] Ma, P-C.; Siddiqui, N.A; Marom, G.; Kim, J-K. *J. Composites, Part A* **2010**, 41, 1345-1367.

[29] Acebal C. C.; Grünhut, M.; Llamas, N. E.; Insausti, M.; Zelená, L.; Sklenářová, H.; Solich, P.; Fernández-Band, B. S. *Microchem. J.* **2016**, 129, 90–97.

[30] Savio, M.; Parodi, B.; Martínez, L. D.; Smichowski, P.; Gil, R. A. *Talanta* **2011**, 85, 245–251.

[31] Rosende, M.; Miró, M.; Segundo, M. A.; Lima, J. L. F. C.; Cerda, V. *Anal Bioanal Chem*. **2011**, 400, 2217–2227.

[32] Boonjob, W.; Miró, M.; Segundo, M. A.; Cerda, V. *Anal. Chem.* **2011**, 83, 5237–5244.

[33] Wu, W.; He, Q.; Jiang, C. *Nanoscale Res. Lett.* **2008**, 3, 397-415.

[34] García-Valverde, M.T.; Galán-Cano, F.; Lucena, R.; Cárdenas, S.; Valcárcel, M. *J. Chromatogr. A* **2014**, 1343, 26-32.

[35] Niu, H.; Wang, Y.; Zhang, X.; Meng, Z.; Cai, Y. *ACS Appl. Mater. Interfaces* **2012,** 4, 286−295.

[36] Cocovi-Solberg, D.; Miró, M. *Anal. Bioanal. Chem.* **2015**, 407, 6227-6233.

[37] Wang, J.-H.; Hansen, E. H.; Miró, M. *Anal. Chim. Acta* **2003**, 499, 139-147.

[38] Quintana, J.B.; Miró, M; Estela, J.M.; Cerda, V. *Anal. Chem.* **2006**, 78, 2832–2840.

[39] Oliveira, H.M.; Segundo, M.A.; Lima, J.L.F.C.; Miró, M; Cerda, V. *J. Chromatogr. A* **2010,** 1217, 3575–3582.

[40] Massart, D. L.; Vandeginste, B. G. M.; Buydens, L.M.C.; De Jong, S.; Lewi, P.J.; Smeyers-Verbeke, J. Handbook of Chemometrics and Qualimetrics: Part A, Elsevier, Amsterdam, 1997, pp. 208-209.

[41] Joint Committee for Guides in Metrology, International Vocabulary of Metrology – Basic and General Concepts and Associated Terms (VIM 3rd edition), JCGM 200:2012.

[42] Menditto, A.; Patriarca, M.; Magnusson, B. *Accred. Qual. Assur.* **2007**, 12, 45-47.

[43] Alcudia-León, M.C.; Lucena, R.; Cárdenas, S.; Valcárcel, M. *Microchem. J.* **2013**, 110, 643–648.

[44] Regueiro, J.; Becerril, E.; García-Jares, C.; Llompart, M. *J. Chromatogr. A* **2009**, 1216, 4693–4702.

[45] Zheng, C.; Zhao, J.; Bao, P.; Gao, J.; He, J. *J. Chromatogr. A* **2011**, 1218, 3830–3836.

[46] Azzouz, A.; Ballesteros, E. *J. Chromatogr. A* **2014**, 1360, 248–257.

[47] Zhao, R.; Yuan, J.; Li, H.; Wang, X.; Jiang, T.; Lin, *J. Anal. Bioanal. Chem.* **2007**, 387, 2911–2915.

[48] Zhao, R.; Wang, X.; Sun, J.; Wang, S.; Yuan, J.; Wang, X. *Anal. Bioanal. Chem.* **2010**, 397, 1627–1633.

[49] Terasaki, M.; Takemura, Y.; Makino, M. *Environ. Chem. Lett.* **2012**, 10, 401–406.

[50] Cheng, C.; Wang, Y.; Ding, W. *Anal. Sci.* **2011**, 27, 197-202.

[51] Baranowska, I.; Magiera, S.; Bortniczuk, K. *Water Sci. Technol.: Water Supply* **2010**, 10, 173-180.

[52] Díaz-Álvarez, M.; Turiel, E.; Martín-Esteban, A. *Int. J. Environ. Anal. Chem.* **2013**, 93, 727-738.

[53] Kim, D.; Han, J.; Choi, Y. *Anal. Bioanal. Chem.* **2013**, 405, 377–387.

[54] Wu, J-L.; Lam, N. P.; Martens, D.; Kettrup, A.; Cai, Z. *Talanta* **2007**, 72, 1650–1654.

[55] Jonkers, N.; Sousa, A.; Galante-Oliveira, S.; Barroso, C.M.; Kohler, H-P.E.; Giger, W. *Sci. Pollut. Res.* **2010**, 17, 834–843.

FIGURE 1

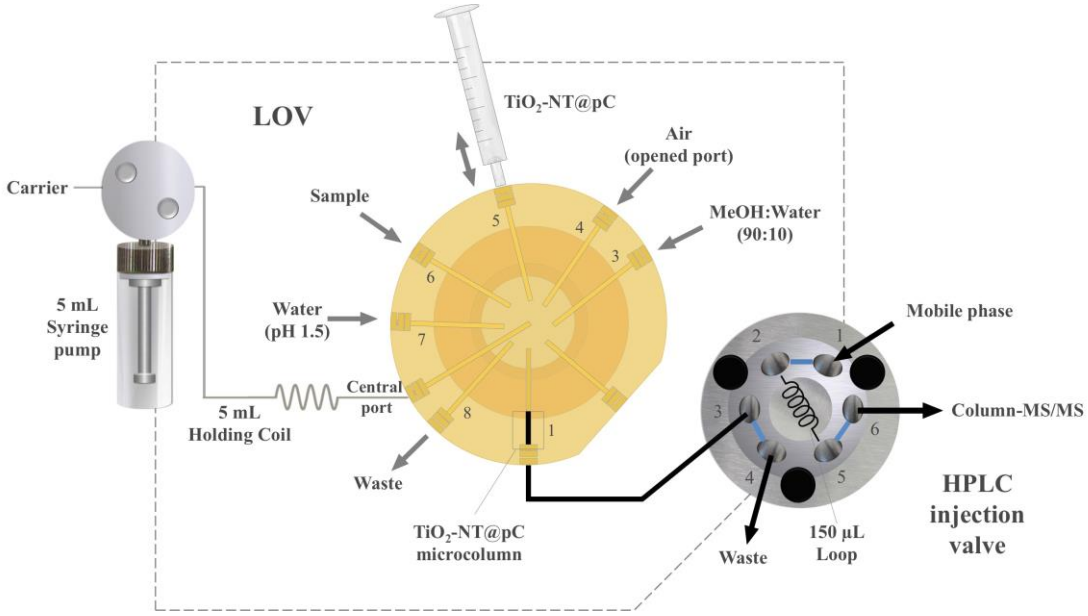
LOV
TiO2-NT@pC
Air
(opened port)
Carrier
Sample
MeOH:Water
(90:10)
5 mL
Syringe
pump
Water
(pH 1.5)
Mobile phase
Central
port
5 mL
Holding Coil
Column-MS/MS
Waste
HPLC
injection
valve
TiO2-NT@pC
microcolumn
Waste
150 µL
Loop

FIGURE 2

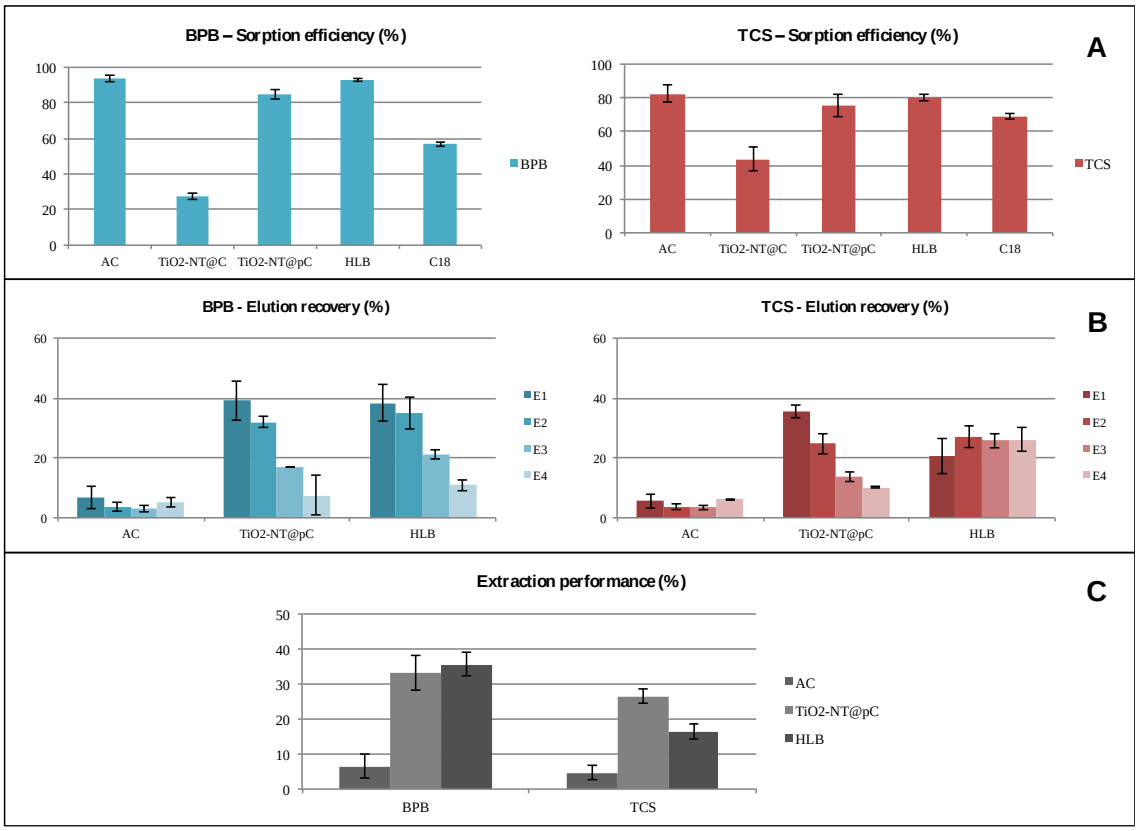
BPB – Sorption efficiency (%)
100
80
60
40
20
0
AC
TiO2-NT@C
TiO2-NT@pC
HLB
C18
BPB
TCS – Sorption efficiency (%)
TCS
A
BPB - Elution recovery (%)
60
40
20
0
E1
E2
E3
E4
TCS - Elution recovery (%)
B
Extraction performance (%)
50
40
30
20
10
0
BPB
TCS
AC
TiO2-NT@pC
HLB
C

FIGURE 3

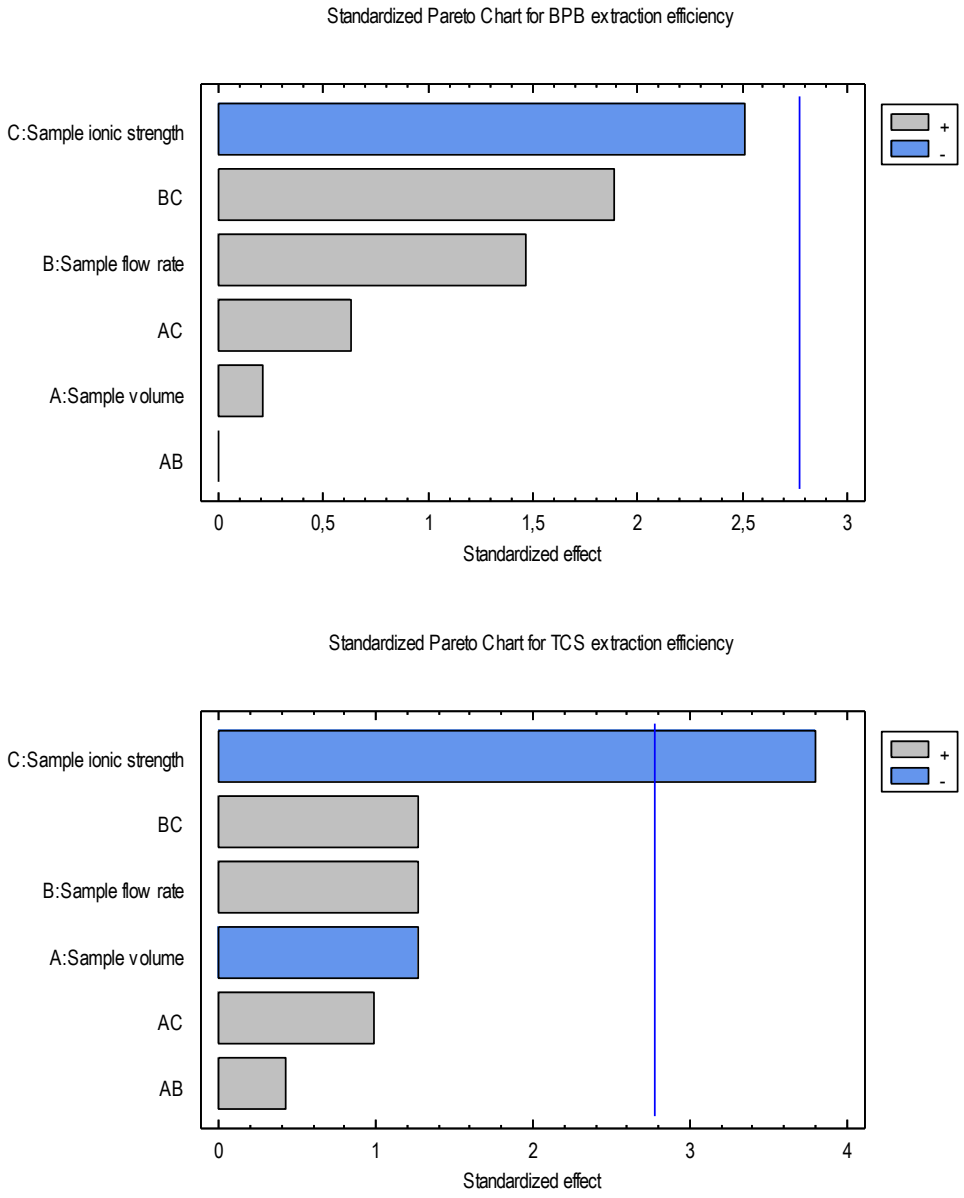
Standardized Pareto Chart for BPB extraction efficiency
C:Sample ionic strength
BC
B:Sample flow rate
AC
A:Sample volume
AB
0
0,5
1
1,5
2
2,5
3
Standardized effect
+
-
Standardized Pareto Chart for TCS extraction efficiency
C:Sample ionic strength
BC
B:Sample flow rate
A:Sample volume
AC
AB
0
1
2
3
4
Standardized effect
+
-

Table 1. Analytical performance of methods reported in the literature for the determination of low abundance parabens and TCS in surface waters using sample processing and chromatographic separation

Reference	Analyte	Matrix	Pretreatment	Equipment	Sample volume (mL)	LOD (ng/L)	RSD (%)	RR (%)
43	MPB, EPB, PBP, BPB	Seawater and swimming pool	Derivatization and magnetically confined hydrophobic nanoparticles microextraction and derivatization	GC-MS	30	23.2–86.1	<7.1	96–106%
44	MPB, EPB, PBP, BPB and TCS	Wastewater, river and swimming pool	SPME and in situ derivatization	GC-MS/MS	10	<17	<12%	>82%
45	TCS	Tap water, river and lake	DLLME-SFO	HPLC-UV	5	100	4.1	84-116
				LC-MS/MS		2	6.2	-
46	MPB, EPB, PBP, BPB and TCS	Tap, well, pond, swimming pool, river and wastewater	SPE and derivatization	GC-MS	100	0.01 (TCS) and 0.07-0.08 (Parabens)	<6.9	90-101
47	TCS	Tap and surface water	HF-LPME and derivatization	GC-MS	15	20	6.9	83.6-114.1
48	TCS	Tap and wastewater	IL-DLPME	HPLC–ESI-MS–MS	5	580	8.8	70-103
49	MPB, EPB, PBP, BPB,	River	SPE and derivatization	GC-MS	1000	0.80-4.2	11	89-104
50	TCS	Surface and wastewater	SPE and derivatization	GC-MS	100	0.4	2-6	95
51	TCS	Surface water	SPE	HPLC-DAD	1000	40	<2	97
52	MPB, iPPB, EPB, PPB, BPB, BzPB,	River, reservoir and sea water	HF-LPME	HPLC-UV	3.5	20-270	<17	…..
53	TCS	River and wastewater	SPME	HPLC-UV	10	1	7	91-105
This work	BPB and TCS	Seawater	LOV-µSPE	LC-MS/MS	5	0.5-0.6	<5.8	97-107

Acronyms: LOD: Limit of detection; RSD: Relative standard deviation; RR: Relative recovery; TCS: Triclosan; MPB: Methylparaben; EPB: Ethylparaben; PPB: Propylparaben;

iPPB: (iso)propylparaben; BPB: Butylparaben; BzPB: Benzylparaben; SPME: Solid phase microextraction; DLLME-SFO: Dispersive liquid–liquid microextraction based on solidification of floating organic droplet; HF-LPME: Hollow fibre-liquid phase microextraction; SPE: Solid phase extraction; IL-DLPME: Ionic liquid dispersive liquid phase microextraction

FIGURE CAPTIONS

Figure 1. Schematic illustration of the µSI-LOV platform as a front end to LC-MS/MS for in-line handling of TiO_2-NT@pC nanomaterials in a disposable format for automatic µSPE of emerging contaminants as demonstrated by the determination of BP and TCS in seawater

Figure 2. Batchwise evaluation of the extraction performance of the TiO_2-carbon hybrid nanomaterials. The analytical procedure is described in SI and illustrated in Fig. S2. (A) Sorption efficiency, (B) Elution capacity (E1-E3: 150 µL, E4: 550 µL) and (C) Extraction performance (sorption × elution efficiency) for the first fraction of eluate (150 µL of eluent)). C18: Octadecyl-chemically modified silica gel; TiO_2-NT@C: carbon-modified titanium dioxide nanotubes; HLB: Divinylbenzene-N-vinylpyrrolidone copolymer (Oasis HLB); AC: Activated carbon; TiO_2-NT@pC: porous carbon-modified titanium dioxide nanotubes

Figure 3. Pareto bar char for multivariate investigation of experimental variables (sample volume, loading flow rate and ionic strength) potentially affecting the extraction efficiency of the automatic LOV-µSPE (TiO_2-NT@pC) method for BPB and TCS.